IJHSR
ijhighschoolresearch.org
■ RESEARCH ARTICLE

Research on Brain Disease Mechanisms: Discovering the Hippocampal Metabolites Resulting Depression Using MALDI Imaging Mass Spectrometry

Jaewon Kang[1], Seoyun Lee, Hoyoung Kang

North London Collegiate School Jeju, Omok-ro 299 Yangcheon-gu, Seoul, 08001, SOUTH KOREA; jaewon200194@gmail.com

ABSTRACT: The research conducted brain metabolite imaging of a depression model (mice) to discover hippocampal metabolites related to depression phenotypes. This identification of hippocampal metabolites was expected to potentially enhance the understanding of the mechanisms underlying depression and brain disorders at a molecular level. The methodology for this research involved MALDI (Matrix-Assisted Laser Desorption/Ionization) Imaging Mass Spectrometry. More specifically, the experimental procedure was as follows. The methods for this research involved MALDI (Matrix-Assisted Laser Desorption/Ionization) Imaging Mass Spectrometry. More specifically, the samples of depressed and non-depressed mice were analyzed using a 9.4T FT-ICR instrument, which simultaneously employs matrix-assisted laser desorption/ionization (MALDI) and electrospray ionization (ESI). These procedures resulted in spatial distribution analysis of molecules in the brain tissue sample, leading to visualization of lipidomics associated with depression phenotypes within the hippocampus. The FTICR-MS analysis revealed mass composition differences in brain tissues between depressed and non-depressed models, particularly noting lipidomic variations in the 700 to 1500 m/z range. Receiver Operating Characteristic (ROC) analysis identified a specific metabolite (314.15363 m/z) predominantly found in non-depressed hippocampal tissue, indicating its possible role in depression. Identifying differential lipidomics offers a path for understanding depression at a molecular level and developing potential therapeutic targets.

KEYWORDS: Medical Biochemistry, Matrix-assisted laser desorption/ionization (MALDI), Receiver Operating Characteristic (ROC), Hippocampal metabolites, Depression phenotype.

■ Introduction

Clinical depression, also known as major depressive disorder (MDD), has emerged as one of the most prevalent psychiatric illnesses in modern times with a high economic burden.[1] Despite its severity, our understanding of the underlying mechanisms of depression remains limited. Consequently, the available treatments for MDD are often inadequate and are somewhat similar to placebos. Therefore, it is crucial to gain a deeper understanding of the underlying mechanisms and molecular changes associated with depression.

The hippocampus has been the site of the most extensive research related to MDD. Previous studies have revealed various structural and functional alterations in the hippocampus of individuals with depression, including reduced volume, impaired neurogenesis, and disrupted synaptic plasticity.[2,3] Some studies have even suggested that lipidomics, such as the hippocampal peroxisome proliferator-activated receptor δ (PPARδ), function as a switch for depression-like behaviors.[4,5] These findings suggest that the hippocampus is intricately involved in the onset of depression. As a result, we hypothesized that depression-related metabolites, or lipidomics, may be found in the hippocampus at level 3, which is the primary focus of this research as it offers key insights into the disease's development.

To test this hypothesis, this research employs MALDI Imaging Mass Spectrometry, using a high-resolution mass spectrometer equipped with a laser microdissection system. We focus on determining the hippocampal lipidomics and metabolites related to depression phenotypes. MALDI Imaging Mass Spectrometry is a powerful mass spectrometry technique that enables the mapping of molecular distribution through the simultaneous use of matrix-assisted laser desorption/ionization (MALDI) and electrospray ionization (ESI).[6] To ensure optimal lipid preservation and MALDI compatibility, brain tissue sections from control and depressed mice will be prepared following established protocols for optimal lipid preservation and MALDI compatibility, including fixation in paraformaldehyde and cryosectioning at 10 µm thickness.[7] To enhance the signal-to-noise ratio and minimize fragmentation during desorption/ionization, we will employ a laser energy-absorbing matrix, such as 9-aminoacridine. Image acquisition will be conducted in positive ion mode with optimized laser power and scanning parameters to acquire high-resolution mass spectra across the hippocampal region.[6] Subsequent data analysis, involving the visualization of spatial distribution for individual lipid species and statistical comparison of metabolite levels between control and depressed groups, will be carried out using specialized software.

This technique offers several advantages, including nondestructiveness and high spatial resolution. It allows for a detailed examination of molecular networks involved in depression pathology. It proves particularly advantageous for visualizing specific lipidomics associated with depression, as it provides

DOI: 10.36838/v7i1.40

spatial distribution analysis of molecules. By scrutinizing the spatial distribution of these molecules, valuable insights into the molecular alterations underlying depression can be obtained.

Previous studies leveraging MALDI imaging to study brain disease mechanisms have demonstrated its potential for identifying crucial molecular changes and providing leads for potential therapeutic targets.[7] Understanding the underlying metabolic dysregulation in depression could lead to the development of targeted therapies aimed at modulating specific lipid pathways or enzymes involved in the biosynthesis or degradation. Furthermore, our findings could contribute to developing noninvasive diagnostic markers for depression based on MALDI-IMS analysis of peripheral tissues, potentially improving early diagnosis and treatment initiation.

However, MALDI imaging also has its limitations. Direct MALDI-TOF analysis of plasma without any sample preparation can lead to severe ion suppression effects. To address this issue, this research utilizes a laser energy-absorbing matrix to minimize fragmentation during the desorption/protonation of sample molecules.[8] Previous studies have successfully employed MALDI-IMS to identify depression-related lipid alterations in rodent models (e.g., reduced phosphatidylcholines and elevated sphingomyelins in the hippocampus). These findings support the potential of our approach to uncover critical molecular signatures associated with depression. While potential limitations, such as inter-animal variability and matrix effects, careful tissue preparation, appropriate controls, and advanced statistical analysis will be employed to ensure the validity and reliability of our results.

Mice were chosen as the experimental model for this study due to their similarities to humans regarding biological traits. Mice, like humans, are mammals and undergo many analogous processes, such as aging, and have similar immune responses to infection and disease. They also share approximately 90% similarity in their genomes with humans.[9] These similarities make mice a valuable model for studying human disorders and diseases, including depression. Additionally, mice offer practical advantages such as a short lifespan, rapid breeding, and well-characterized brain anatomy. Therefore, using mice as the primary experimental model in this research is reasonable.

In conclusion, the overall research on determining the hippocampal lipidomics and metabolites related to depression phenotypes using MALDI imaging. The findings are expected to enhance our overall understanding of brain disease mechanisms while suggesting a potential therapeutic target for future depression treatments.

Methods

Development of depression mouse model:

C57BL/6 mice from Orient Bio were bred to obtain offspring for the study. Each newborn mouse was injected with tricyclic antidepressant clomipramine at a dose of 20 mg/kg every 24 hours from postnatal day 6 to 22. To create a control group, another group of mice was administered the equivalent volume of saline for the same time intervals. After this injection period, only male mice were selected, considering the difference in proneness to stress in male and female mice.

Behavioral experiments were conducted after 8 weeks, and experimental models were born. The test mainly involved introducing the C57BL/6 mice as an intruder into a home cage of CD1 mice, recording the duration of the C56BL/6 fighting against the resident's attack. Exhibition of immobility or contact with the CD1 was used to indicate that the modified C57BL/6 mice were depressed.

Cardiac perfusion:

To perform the cardiac perfusion, an anesthetic mixture (ketamine + xylazine) was injected intraperitoneally into the-depression model (Figure 1). The mouse's four limbs were then secured, ensuring the abdomen was fully extended, and the stomach positioned upwards. A lateral incision below the sternum and rib cage exposed the diaphragm and liver (Figure 2). The diaphragm was cut along the side in contact with the abdominal skin using iris scissors to avoid damaging internal organs. With partial incisions, the central bone of the rib cage was bent upwards with a clamp to expose the thoracic cavity containing the heart.

While holding the heart with forceps, a cannula was inserted into the left ventricle. The tubing of the peristaltic pump was attached to solutions containing 50 ml of each pre-prepared 1X PBS and 4% PFA. A small incision was made in the right atrium. The peristaltic pump was subsequently turned on to replace blood in the circulatory system with PBS. The pump was stopped once the liver color of the mouse turned white, ensuring all the blood had been drained from the body.

Figure 1: Injection of anesthetic mixture.

Figure 1: Mouse's thoracic cavity.

Dissection (brain extraction):

To extract the brain from the mouse model, the proximal end of the neck and vertebrae from the occipital bone of the skull were cut using scissors. A scalpel was then used to draw a midline and peel off the scalp. 2-3 midline cuts were then made on the skull with the scalpel, creating shallow fractures. The muscles and fat at the back of the skull were trimmed using scissors, exposing the white brainstem and cerebellum. The scissors were then inserted into the brainstem slightly to cut the occipital skull in a cross-shaped pattern. By inserting forceps between the skull and the brain, the skull was gently twisted outward to remove it (Figure 3). Spatula was used to

DOI: 10.36838/v7i1.40

sever the optic nerves beneath the brain before the removal of the brain.

Figure 3: Craniotomy of mouse's skull.

Tissue preparation:

To prepare the brain tissue for cryostat sectioning, a piece of aluminum foil boat floated on liquid nitrogen while the tissue was placed inside. After 5 seconds, a spatula transferred liquid nitrogen inside the boat. The method was repeated every 5 seconds until the tissue was covered entirely (Figure 5). The tissue was placed inside a plastic tube and stored at −80˚C for rapid freezing (Figure 6). The process is summed up in Figure 4.

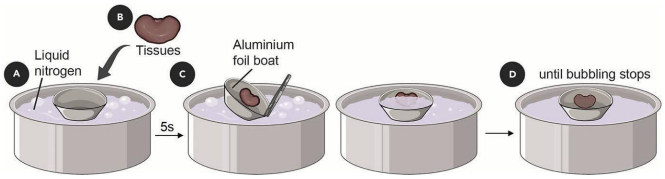

Figure 4: Tissue preparation, rapidly freezing brain tissue in liquid nitrogen[10]

Figure 5: Rapid freezing using liquid nitrogen.

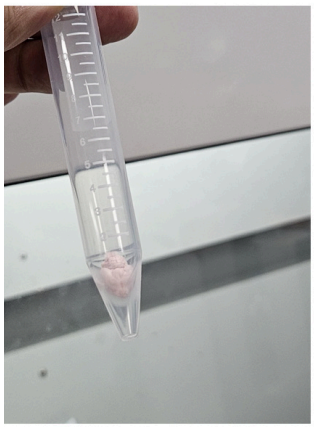

Figure 6: Frozen brain tissue sample.

Cryostat sectioning[11]:

The brain sample was added and positioned on a circular cryostat block so the mouse's frontal lobe faced upwards. A mold was created by rolling a film into a cylinder shape and placing it over the cryostat block. The mold containing the sample was filled with OCT (Optimal Cutting Temperature) and frozen inside the cryostat chamber (-25 degrees) until the block turned opaque. The film paper was removed, and the block (the disk) was placed in the mounting area.

The block was initially sectioned to a thickness of 100μm by operating the cutting handwheel at a slow stroke. Once the upper part of the brain sample was visible, the thickness was adjusted to 15μm, and sectioning was continued until level 3 of the mouse's brain (Figure 8) was visible (Figure 7). The anti-roll cover was then lowered to create another slice.

After removing the anti-roll cover, the slice was moved to the lower area of the stage and unrolled using a brush (Figure 9). The ITO slide was then lowered over the slice

Figure 7: Level 3 section of mouse's brain.

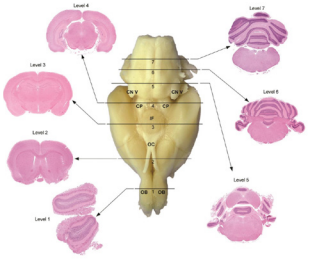

Figure 8: Seven transverse (coronal) hematoxylin and eosin–stained sections corresponding to levels based on anatomic target landmarks.[12]

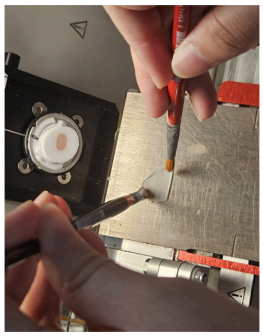

Figure 9: Unrolling brain tissue.

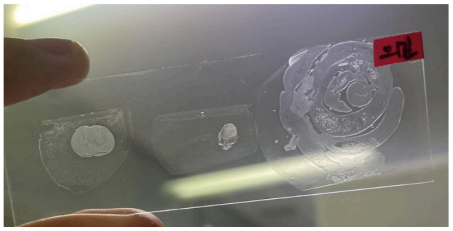

Figure 10: · Brain tissue sample, heart sample, and intestine sample on ITO glass slide.

Sample preparation for MALDI-IMS:

To prepare the sample for MALDI-Imaging Mass Spectrometry, 180 ml of ACN was mixed with 20 ml of 0.1% TFA solution to create 200 ml of 90% ACN +10% H_2O + 0.1%

TFA solution. 30 mg of DHB was dissolved into the solution to produce a 15mg/ml matrix solution.[13] The tissue was placed within the spray chamber and fastened to the TM Sprayer using tape.

The plate was selected using the TM Sprayer control software, and the spray area was adjusted so the tissue would be thoroughly sprayed with the matrix solution (Figure 11). By clicking the column next to the left of the method, the method using DHB as its sprayer was selected (Figure 12). The parameters of the HTX TM-sprayer were adjusted to achieve a homogeneous matrix crystal deposition; the temperature was adjusted to 60 degrees, the gas flow rate to 3 l/min, and the pressure to 10 psi (Table 1).[7]

After switching the valve to the LOAD position, a syringe loaded the DHB matrix solution into the loop. The machine was started after adjusting the matrix volume to 5 ml in the Cycle tab. The valve was switched to SPRAY, and CONTINUE was clicked when prompted. At the end of the Cycle, the valve was switched back to LOAD, and the slide was removed from the HTX TM-sprayer.

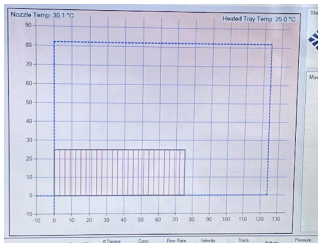

Figure 11: Adjusting spray area.

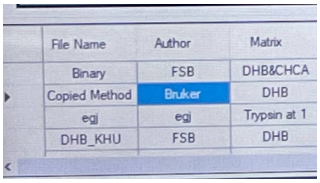

Figure 12: Choosing method

Table 1: Adjusting parameters including temperature (°C), number of passes (count), concentration (mg/ml), flow rate (ml/min), velocity (mm/min), track spacing (mm), pattern, pressure (psi), gas flow rate (l/min), gas flow rate (l/min), drying time (s), and nozzle height (mm).

	Temp (°C)	# Passes (Count)	Conc. (mg/ml)	Flow Rate (ml/min)	Velocity (mm/min)	Track Spacing (mm)	Pattern	Pressure (psi)	Gas Flow Rate (l/min)	Drying Time (s)	Nozzle Ht. (mm)
90% ACN +10% H2O + 0.1% TFA	60	14	15	0.125	1200	3	CC	10	2	0	40

MALDI-TOF MS and MS/MS:

For MALDI time of Flight (MALDI-TOF) mass spectrometry and Tandem mass spectrometry (MS/MS), the tissue slide was transferred to the MALDI mass spectrometer using the MTP slide adapter. Utilizing the MALDI-TOFSpectrometer, we acquired IMS spectra in positive and negative ion reflector modes. The mass range was set between 0 and 3000 m/z with average signals from 500 laser shots with a frequency of 200. The peptide calibration standard of 800-3200 was used for external calibration before each data acquisition. Baseline subtraction for all obtained spectra was carried out, and the data analysis software (Imagingflex, Scils lab, etc.) was used to obtain density maps of the phospholipid species. The distribution of lipids at a spatial resolution of 200 µm per image pixel was compared using (Figure 13).

MS/MS analysis was performed on selected phospholipids to characterize further and confirm identified phospholipids.

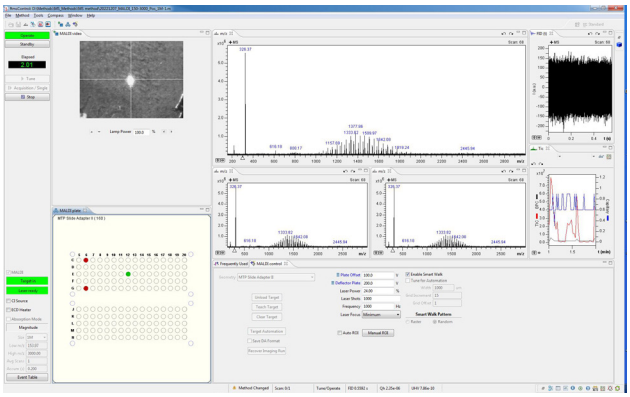

Figure 13: Comparison of lipids at a spatial resolution of 200 µm per image pixel using.

Results

The mass of 964,408 ionization points was determined by the Fourier Transform Ion Cyclotron Resonance Mass Spectrometry (FTICR-MS) analysis. Employing Mass Spectrometry Imaging (MSI), it was indicated that notable peaks in intensity were observed within a 700-1000 m/z range (Figure 14), suggesting a specific range for the components of the hippocampal region. However, previously imperceptible peaks from 200-500 m/z and 1000-1500 m/z were found to generate a skyline spectrum region (Figure 15). This suggested that meaningful hippocampal lipidomics could be seen from the initial 7000-1000 m/z range. Therefore, the mass range for implying the Receiver Operating Characteristic (ROC) algorithm was expanded to 200-1500 m/z.

The ROC algorithm was also used to compare depressed and non-depressed models. The algorithm visualized the spatial distribution of molecules in each brain tissue, particularly those that exhibited a significant intensity difference between the two models, as MALDI images. Figure 16 displays the top 50 substances with a higher intensity in the non-depressed model that meet the condition. Figure 17 illustrates the top 50 more concentrated substances within the depressed model.

According to the generated MALDI images, the mass of a hippocampal component reflecting the highest difference in each model was identified as 314.15363 m/z. Specific to this mass, Figure 18 illustrates a relatively more intense red coloration within the hippocampal region of the non-depressed model. In contrast, this region appears yellow to blue in the depressed model. This observation implies that the 314.15363 m/z substance is more likely to be found in the non-depressed hippocampus than in a depressed hippocampus - suggesting that its secretion might have been inhibited under depressive conditions. In other words, the identified 314.15363 m/z molecule can potentially be a hippocampal metabolite that functions as a switch for depression.

DOI: 10.36838/v7i1.40

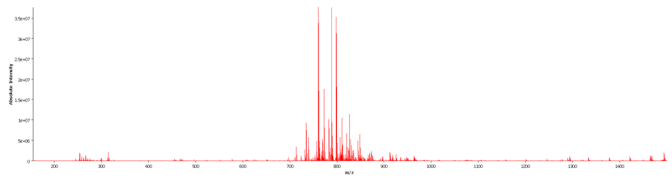

Figure 14: The mean spectrum of regions exhibits absolute intensity along the mass-to-charge ratio (m/z). The m/z value range with notable peaks indicates the specific range for the components of the hippocampal region.

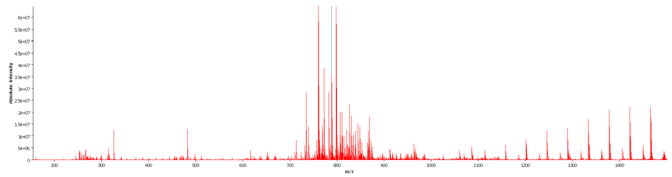

Figure 15: Skyline spectrum with enhanced sensitivity, highlighting unperceived hippocampal components from Figure 15.

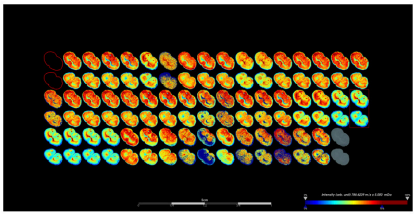

Figure 16: MSI analysis, ROC top 50 higher-intensity substances in the non-depressed model. Colors closer to red indicate high intensity, while colors closer to blue indicate low intensity, showing regions of upregulated or downregulated expression.

The upregulated or downregulated substances could indicate hippocampal metabolites responsible for the switch for depression.

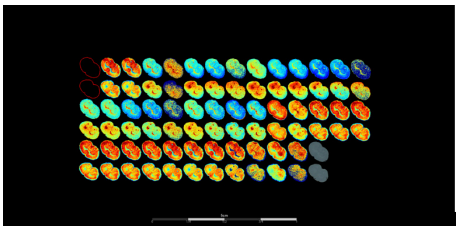

Figure 17: MSI analysis, ROC top 50 substances in higher intensity at the depressed model Colors closer to red indicate high intensity. In contrast, colors closer to blue indicate low intensity – showing regions of upregulated or downregulated expression. The upregulated or downregulated substances could indicate hippocampal metabolites responsible for the switch for depression.

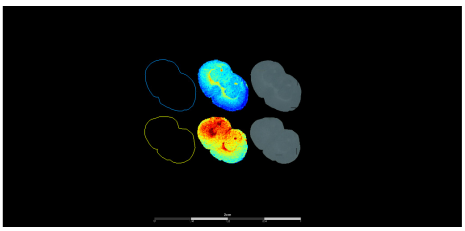

Figure 18: The results of the MSI analysis for the substance corresponding to 314.15363 m/z visualize the compound's spatial distribution. The areas highlighted in red indicate a high concentration of the composition.

Discussion

Despite the meaningful results, the number of experimental subjects must be considered for its generalization. Due to environmental constraints, only a single case (n=1) was analyzed for each depressed and non-depressed mouse within this research. The limited quantity of datasets to confirm the result leaves a possibility for the specificity of data; the suppression of 314.15363 m/z metabolite under depression might only be present in the specific mice used in this research. Multiple statistical methodologies were involved to compensate for the limitation, particularly Skyline AUC, PCA, pLSA, and Heatmap.

However, considering the research's limitations, increasing the number of analyzed mice models, ideally to at least 6, would be required for a definite conclusion.

Nevertheless, the potential and value of the results obtained from this research remain promising. This research successfully mapped the spatial distribution of hippocampal lipidomics of both depressed and non-depressed models. The visual comparison between the results has specified the mass of a potential substance that is suppressed during depression: 314.15363 m/z. This aligns with similar reports of lipidomic dysregulation in the brain during depression, such as suppression of phosphatidylcholine(PC) or phosphatidylethanolamine(PE).[14] Given the ability of specific bioactive lipids to control emotions and mood-related manifestations, the correlation between 314.15363 m/z lipidomic and depression appears plausible.[15] With further experimental refinements—such as increasing the number of experimental subjects and improving precision—this lipidomic could be definitively identified, providing a potential therapeutic target in treating depression.

Conclusion

The research aimed to practice finding a decisive hippocampal metabolite for depression, either for its suppression or causation. To accomplish this, MALDI images of the hippocampus of both depressed and non-depressed mice were generated. Using the ROC algorithm, the images were compared in terms of composite substance intensity. The mass of a hippocampal component with the highest intensity difference in each model was subsequently identified as 314.15363 m/z – more frequently found in the non-depressed model than the depressed model. Despite the potential of this substance, which has a corresponding mass, to function as a suppressor for depression, the lack of quantity in data provides a hurdle for a definite conclusion. However, the research provides a promising foundation for future research, offering a general understanding of a molecular neuroscientific approach to depression etiopathogenesis.

Acknowledgments

Jaewon Kang, Hoyoung Kang, and Seoyun Lee contributed equally to this work. The laboratory area was provided by KBSI (Korea Basic Science Institute).

References

1. Li, Z.; Ruan, M.; Chen, J.; Fang, Y. Major Depressive Disorder: Advances in Neuroscience Research and Translational Applicatio ns. Neuroscience Bulletin 2021, 37 (6). https://doi.org/10.1007/

s12264-021-00638-3.
2. Malykhin, N. V.; Carter, R.; Seres, P.; Coupland, N. J. Structural Changes in the Hippocampus in Major Depressive Disorder: Co ntributions of Disease and Treatment. Journal of psychiatry & neu roscience: JPN 2010, 35 (5), 337–343. https://doi.org/10.1503/jp n.100002.
3. Finkelmeyer, A.; Nilsson, J.; He, J.; Stevens, L.; Maller, J. J.; Moss, R. A.; Small, S.; Gallagher, P.; Coventry, K.; Ferrier, I. N.; McAllis ter-Williams, R. H. Altered Hippocampal Function in Major De pression despite Intact Structure and Resting Perfusion. Psycholo gical Medicine 2016, 46 (10), 2157–2168. https://doi.org/10.101 7/s0033291716000702.
4. Müller, C. P.; Reichel, M.; Mühle, C.; Rhein, C.; Gulbins, E.; Ko rnhuber, J. Brain Membrane Lipids in Major Depression and Anx iety Disorders. Biochimica et Biophysica Acta (BBA) - Molecular and Cell Biology of Lipids 2015, 1851 (8), 1052–1065. https://doi.org/10.1016/j.bbalip.2014.12.014.
5. Chen, F.; Yu, X.; Meng, G.; Mei, Z.; Du, Y.; Sun, H.; Reed, M. N.; Kong, L.; Suppiramaniam, V.; Hong, H.; Tang, S. Hippocampal Genetic Knockdown of PPARδ Causes Depression-like Behavior s and Neurogenesis Suppression. International Journal of Neurop sychopharmacology 2019, 22 (6), 372–382. https://doi.org/10.1093/ijnp/pyz008.
6. MALDIImaging.www.bruker.com. https://www.bruker.com/en/ applications/academia-life-science/imaging/maldi-imaging.html.
7. CMU - Carnegie Mellon University USER MANUAL HTXT M-sprayer. https://www.cmu.edu/chemistry/facilities/cma/pdfs/ htx-spray_user_manual.pdf
8. HTX TM-SprayerTM MALDI Sample Preparation System. htt ps://static1.squarespace.com/static/55eae94ae4b08810efb9cd87/ t/5c13cb22b8a045c20080248 1/1544801064703/HTX_TM-Spr ayer_Brochure+D3.pdf.
9. Breschi, A.; Gingeras, T. R.; Guigó, R. Comparative Transcriptom ics in Human and Mouse. Nature Reviews Genetics 2017, 18 (7), 425–440. https://doi.org/10.1038/nrg.2017.19.
10. Wang, F.; Naowarojna, N.; Zou, Y. Stratifying Ferroptosis Sensiti vity in Cells and Mouse Tissues by Photochemical Activation of Lipid Peroxidation and Fluorescent Imaging. STAR Protocols 20 22, 3 (2), 101189. https://doi.org/10.1016/j.xpro.2022.101189.
11. Revilla, V.; Jones, A. Cryostat sectioning of brains. Science Direc t. https://www.sciencedirect.com/science/article/abs/pii/S007477 4202470523 (accessed 2024-07-14).
12. Bolon, B.; Garman, R. H.; Pardo, I. D.; Jensen, K.; Sills, R. C.; R oulois, A.; Radovsky, A.; Bradley, A.; Andrews-Jones, L.; Butt, M. ; Gumprecht, L. STP Position Paper. Toxicologic Pathology 2013, 41 (7), 1028–1048. https://doi.org/10.1177/0192623312474865.
13. Shanta, S. R.; Zhou, L.-H.; Park, Y. S.; Kim, Y. H.; Kim, Y.; Kim, K. P. Binary Matrix for MALDI Imaging Mass Spectrometry of Phospholipids in Both Ion Modes. Analytical Chemistry 2011, 8 3 (4), 1252–1259. https://doi.org/10.1021/ac1029659.
14. Costa, A.P., Dijr, van, Talati, A., Weissmann, M.M. and McIntire , L.B. (2021b). 48352 Mechanisms Underlying Lipidomic Chang es in Major Depressive Disorder. Journal of Clinical and Translati onal Science, [online] 5(s1), pp.99–100. doi:https://doi.org/10.10 17/cts.2021.656.Chiurchiù, V. and Maccarrone, M. (2016). Bioact ive lipids as modulators of immunity, inflammation and emotions. Current Opinion in Pharmacology, 29, pp.54–62. doi:https://doi. org/10.1016/j.coph.2016.06.005.
15. Chiurchiù, V. and Maccarrone, M. (2016). Bioactive lipids as mo dulators of immunity, inflammation and emotions. Current Opini on in Pharmacology, 29, pp.54–62. doi:https://doi.org/10.1016/j. coph.2016.06.005.

Authors

Jennifer Jaewon Kang NLCS 2026
* E-mail: jaewon200194@gmail.com
Seoyun Lee Chadwick International School 2026
* E-mail: shinelee757@gmail.com
Hoyoung Kang St John's School 2026
*E-mail: 2026hoyoungkang@gmail.com

DOI: 10.36838/v7i1.40